The 8th European Congress on Computational Methods in Applied Sciences and Engineering
ECCOMAS Congress 2022
5–9 June 2022, Oslo, Norway

# TWO-SCALE ASYMPTOTIC HOMOGENIZATION IN A MEMS AUXETIC STRUCTURE FOR OVER ETCH IDENTIFICATION

**David Faraci[1], Alessandro Nastro[2], Valentina Zega[1] and Claudia Comi[1]**

[1] Department of Civil and Environmental Engineering
Politecnico di Milano
Piazza Leonardo da Vinci 32, 20133 Milan, Italy
e-mail: david.faraci@polimi.it

[2] Department of Information Engineering
University of Brescia
25123 Brescia, Italy

**Key words:** MEMS, periodic auxetic structure, over etch, asymptotic homogenization

**Abstract.** The development and optimization of Micro electro-mechanical systems (MEMS) devices, due to their small size scale, require testing and precise characterization. As an example, over etch, which is the deviation between the designed masks and the effective dimensions of the suspended parts, strongly influences the performances of MEMS; therefore, to predict the correct functioning of the device its actual value must be carefully identified. In this work, we propose an efficient, time-saving tool to identify fabrication imperfections in MEMS devices. In particular, we replace the complex geometry of a MEMS mechanical filter with an equivalent homogeneous medium, whose linear-elastic effective properties are evaluated employing two-scale asymptotic homogenization and we identify the over etch by minimizing the relative error between experimental data and corresponding predictions obtained for different combinations of over etch.

## 1 INTRODUCTION

Micro electro-mechanical systems (MEMS) are attracting increasing attention thanks to the large variety of possible applications spanning from the consumer market to the automotive industry or from the virtual/augmented reality to the internet of things [1, 2]. The design and fabrication of such devices require reliable analytical or numerical models able to predict the correct function of the device, but also extremely precise fabrication processes. Unknown mechanical or geometrical parameters can indeed compromise the predictivity of the models and consequently the performances of MEMS devices.

In the literature, several approaches able to assess these type of uncertainties through the exploitation of experimental methods and/or relevant modelling strategies have been proposed so far. As an example, we can mention techniques that rely on surface inspections through optical/scanning electron microscopy [3] or laser interferometry [4]. These approaches are usually too invasive especially if devices are encapsulated in vacuum and the package is not transparent.

Other approaches are based on tension and bending deformations of a specimen [5, 6] or on the inverse identification of the unknown parameters through the combination of experiments and finite element models. The last strategy is very promising, but has huge computational costs especially if the geometry is complex and thin flexible elements are present. To overcome such limitations, in [7, 8] standard electrical probing is combined with transitional Markov chain Monte Carlo (TMCMC) analysis to identify geometrical and material properties of polysilicon films. The high computational cost deriving from the use of Finite Elements simulations in TMCMC analyses has been indeed strongly reduced through a parametric model order reduction method based on a hybrid use of proper orthogonal decomposition and kriging metamodeling.

In this work, we propose an hybrid modelling reduction strategy based on the combination of an analytical model and an homogenization technique. A proper optimization procedure is employed to identify geometrical uncertainties, by minimizing the difference between modelling predictions and data coming from standard experimental tests on a fabricated MEMS. Among various geometrical parameters which can be affected by uncertainties, we focus in particular on the over etch, which is due to the chemical attack during the fabrication process. The over etch usually spans from tenth of microns to some microns, depending on the employed fabrication process, and strongly influences the performances of MEMS devices.

In particular, here we focus on the innovative MEMS electrically-tunable mechanical filter recently proposed by co-authors in [9]. A schematic view of the mechanical structure is shown in Figure 1a: it embeds a deformable structure made of a periodic repetition of an auxetic unit cell firstly proposed in [10] and four external frames suspended through folded springs. A close-up view of the unit cell is reported in Figure 1b. Electrostatic actuation and readout are performed through electrodes located inside the left ($F_D$) and right ($F_S$) frames (see Figure 1c). According to the parallel-plate capacitor scheme, when a Direct-Current (DC) voltage difference is applied between the stator $D$ or $S$ (electrodes fixed on the substrate) and the rotor $R$ (external frames of the structure), an electrostatic force is generated and the mechanical structure is actuated.

## 2 TWO-SCALE ASYMPTOTIC HOMOGENIZATION

The idea of the homogenization technique here proposed is to substitute the inner deformable part of the MEMS filter with a continuum material of equivalent properties, thus reducing the mesh complexity and consequently the computational costs of numerical simulations.

### 2.1 Homogenization approach

The central region $\Omega$ of the MEMS mechanical filter shown in Figure 1a is here considered as a single-phase periodic structure, of characteristic size $L$, which is constructed by the periodic repetition of the square unit cell $Y^\epsilon$ of side $\ell$, shown in Figure 1b. Note that only a subset $Y_m^\epsilon \subset Y^\epsilon$ is filled by the material. Under the hypothesis of scale separations, i.e., when the ratio $\epsilon = \ell/L \ll 1$, the properties of the periodic media can be described through homogenization techniques.

The linear-elastic static behaviour of the periodic structure, in absence of body forces, is governed by the equilibrium equations

$$\operatorname{div}\left[\mathbb{D}^\epsilon : \boldsymbol{\varepsilon}(\mathbf{u}^\epsilon)\right] = \mathbf{0} \qquad \text{in } \Omega, \tag{1}$$

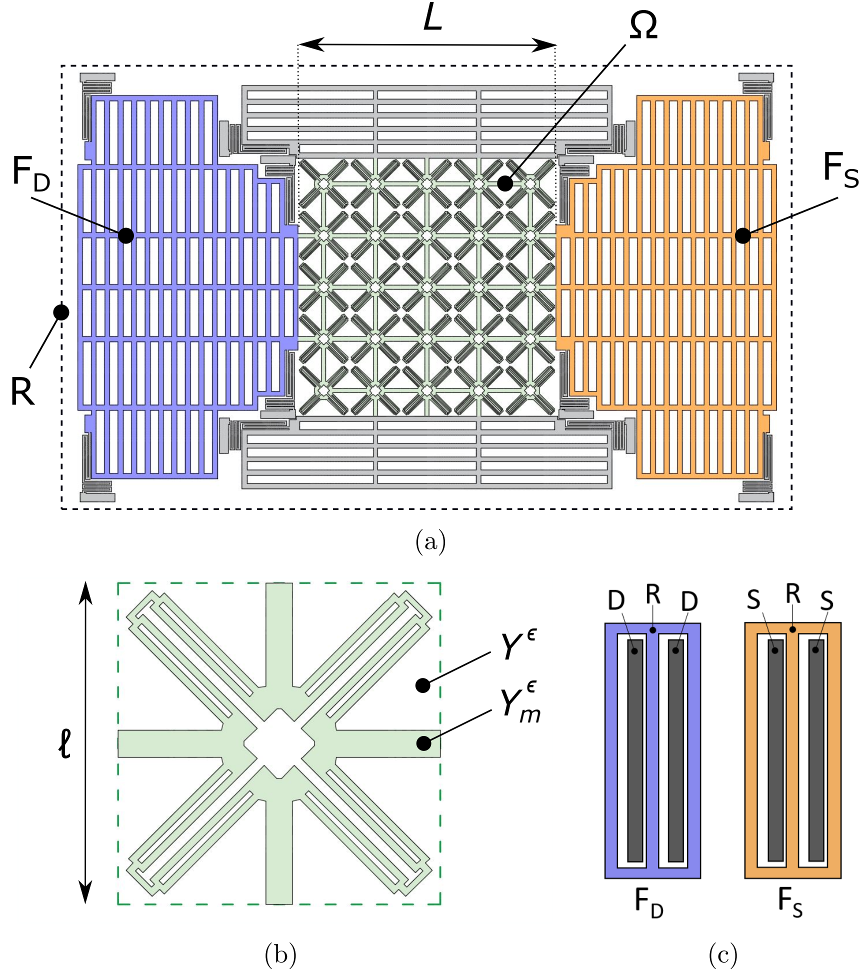


Figure 1: (a) Schematic view of the MEMS structure under study. Close-up view of the (b) unit cell and of the (c) electrostatic actuation/readout schemes.

where $\mathbf{u}^\epsilon$ is the displacement field, $\boldsymbol{\varepsilon}$ is the symmetric part of the displacement gradient and $\mathbb{D}^\epsilon$ is the elastic stiffness tensor of the constituent material, which is periodically varying. Assuming for simplicity isotropic behavior, the elastic stiffness reads

$$\mathbb{D} = 2\mu^\epsilon \mathbb{I} + \lambda^\epsilon \mathbf{I} \otimes \mathbf{I}, \tag{2}$$

being $\lambda^\epsilon$ and $\mu^\epsilon$ the first and second Lame's constants of the material.

The homogenized effective properties of the periodic structure are obtained by studying the asymptotic limit $\epsilon \to 0$ of the equation (1). Indicated with $\mathbf{x}$ the macroscopic variable, we introduce the fast variable $\mathbf{y} = \mathbf{x}/\epsilon$ and the re-scaled unit cells $Y = Y^\epsilon/\epsilon$ and $Y_m = Y_m^\epsilon/\epsilon$. According to the two-scale asymptotic technique, we assume the following ansatz

$$\mathbf{u}^\epsilon(\mathbf{x}) = \mathbf{u}^0\left(\mathbf{x}, \frac{\mathbf{x}}{\epsilon}\right) + \epsilon \mathbf{u}^1\left(\mathbf{x}, \frac{\mathbf{x}}{\epsilon}\right) + \dots \qquad \text{and} \qquad \mathbb{D}^\epsilon(\mathbf{x}) = \mathbb{D}\left(\frac{\mathbf{x}}{\epsilon}\right), \tag{3}$$

where the fields $\mathbf{u}^i(\mathbf{x}, \mathbf{y})$ and $\mathbb{D}(\mathbf{y})$ are defined on $\Omega \times Y_m$ and are periodic with respect the fast variable. Substituting (3) into equation (1), one obtain a sequence of differential problem to be solved for each order of the parameter $\epsilon$.

Following the standard arguments of homogenization theory, see e.g. [11, 12, 13], one can deduce that the first term of expansion (3) does not depend on $\mathbf{y}$, i.e., $\mathbf{u}^0(\mathbf{x}, \mathbf{y}) = \mathbf{U}^0(\mathbf{x})$ in $\Omega \times Y_m$, and that the homogenized equilibrium equation of the periodic body is

$$\mathrm{div}_{\mathbf{x}} \left[\mathbb{D}^0 : \boldsymbol{\varepsilon}_{\mathbf{x}}(\mathbf{U}^0)\right] = \mathbf{0} \qquad \text{in } \Omega, \tag{4}$$

where $\mathbb{D}^0$ is the effective stiffness tensor. The homogenized stiffness components can be evaluated through

$$D^0_{ijhk} = \frac{1}{|Y|} \int_{Y_m} \left[\boldsymbol{\varepsilon}_{\mathbf{y}}(\boldsymbol{\chi}^{ij}) + \mathbf{e}_i \odot \mathbf{e}_j\right] : \mathbb{D} : \left[\boldsymbol{\varepsilon}_{\mathbf{y}}(\boldsymbol{\chi}^{hk}) + \mathbf{e}_h \odot \mathbf{e}_k\right] \, d\mathbf{y}, \tag{5}$$

where $\mathbf{e}_i$ is the unit vector in the $i-$th direction and the functions $\boldsymbol{\chi}^{ij}(\mathbf{y})$ are solutions of the following problems

$$\begin{cases} \mathrm{div}_{\mathbf{y}} \left[\mathbb{D} : \boldsymbol{\varepsilon}_{\mathbf{y}}(\boldsymbol{\chi}^{ij})\right] = \mathbf{0} & \text{in } Y_m \\ \boldsymbol{\chi}^{ij} \quad \text{periodic} & \text{on } \partial Y_m \cap \partial Y \\ \left[\mathbb{D} : \left(\boldsymbol{\varepsilon}_{\mathbf{y}}(\boldsymbol{\chi}^{ij}) + \mathbf{e}_i \odot \mathbf{e}_j\right)\right] \cdot \mathbf{n} \quad \text{anti-periodic} & \text{on } \partial Y_m \cap \partial Y \\ \left[\mathbb{D} : \left(\boldsymbol{\varepsilon}_{\mathbf{y}}(\boldsymbol{\chi}^{ij}) + \mathbf{e}_i \odot \mathbf{e}_j\right)\right] \cdot \mathbf{n} = \mathbf{0} & \text{on } \partial Y_m \setminus \partial Y \end{cases}. \tag{6}$$

The cell problems (6) are elastic problems in which uniform eigenstrains are imposed within the unit cell of the periodic material. Their solutions are determined up to a rigid body motion, which can be fixed by enforcing the additional constraints

$$\int_{Y_m} \boldsymbol{\chi}^{ij}(\mathbf{y}) \, d\mathbf{y} = \mathbf{0}. \tag{7}$$

### 2.2 Validation of the homogenized properties

The homogenization technique described in the previous section, is here employed as a fast and efficient tool for the numerical evaluation of the linear-elastic equivalent stiffnesses $k_{eq}$ of the $F_S/F_D$ frames when they are subjected to uniform horizontal forces for different values of the over etch, which is assumed to be uniform on the whole MEMS. This is computed by finite element analysis, carried out with the commercial software COMSOL Multiphysics, by taking the ratio between the uniformly applied horizontal force on the frame and its average horizontal displacement.

The validity of the homogenization method, i.e., the replacement of the inner auxetic core with a homogeneous media of effective properties provided by (5), is first checked in the case of the MEMS nominal geometry (zero over etch).

The mesh employed for the real model of the MEMS is shown in Figure 2a, on the left, and it is composed of 1,600,000 serendipity quadratic tetrahedral elements. Note that the anchoring springs and the branches of the auxetic cells require a fine discretization to correctly reproduce their flexural behaviour, which may represent a huge computational burden.

When the inner auxetic core is replaced by an equivalent homogenized media, a coarser mesh can be used reducing the number of elements to 600,000, see Figure 2a on the right (in blue).

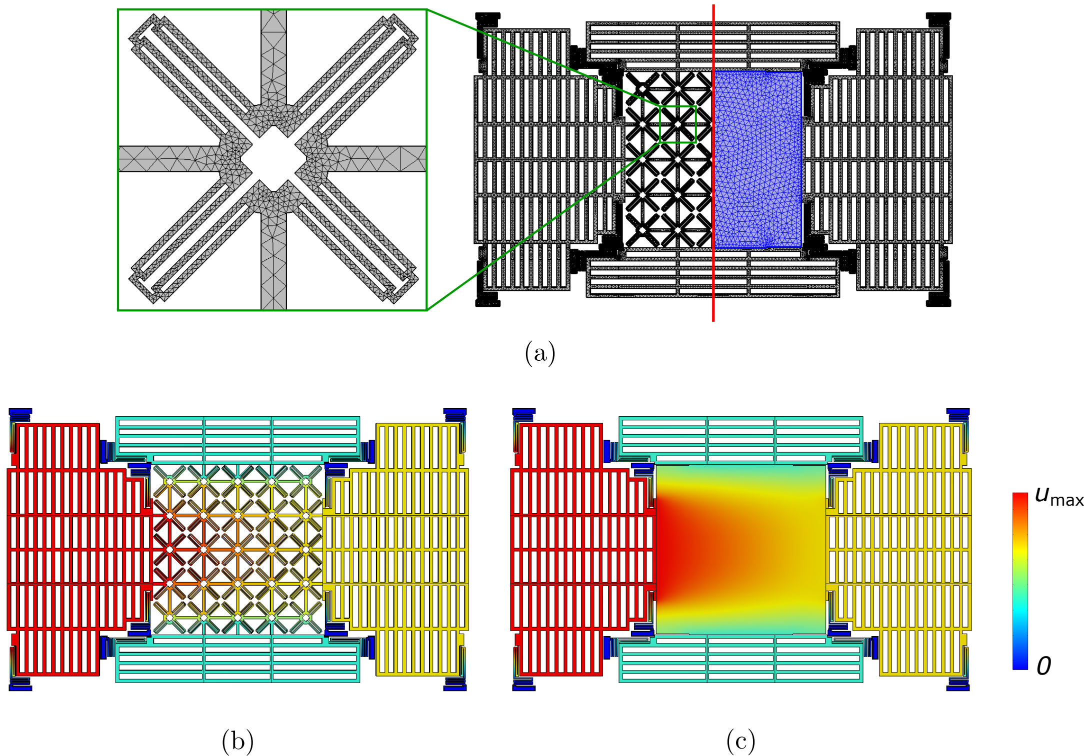


Figure 2: (a) Meshed real model (left) and the homogenized one (right); contours of the horizontal displacement of the real model (b) and of the homogenized one (c)

Figure 2b and Figure 2c show the contours of the horizontal displacements obtained through the numerical simulation with the real auxetic geometry and the homogenized one, respectively. The frame equivalent stiffness $k_{eq}$ estimated through the homogenization technique shows a discrepancy of 1.5% with respect to its counterpart computed through full order finite elements simulation, while the computational time is reduced by 90%. A similar time-saving gain of the homogenization is expected for different values of the over etch.

The same good agreement is found for different values of over etch in the range 0-0.5$\mu$m.

## 3 OVER ETCH IDENTIFICATION

### 3.1 Experimental tests

To experimentally characterize the electrostatically tunable mechanical MEMS filter shown in Figure 1 and thus collecting the data needed for the over etch identification procedure here proposed, tests in the static regime have been performed on two nominally equal devices (named A and B in the following).

Figure 3a shows a scheme of the experimental setup implemented to perform such measurements. The capacitance $C_{SR}$ between terminals $S$ and $R$ and the capacitance $C_{DR}$ between terminals $D$ and $R$ have been measured exploiting the impedance meter HP4194A, by applying a proper sinusoidal probing signal $v_p(t)$ and a tunable DC-bias voltage $V_b$. The experimental

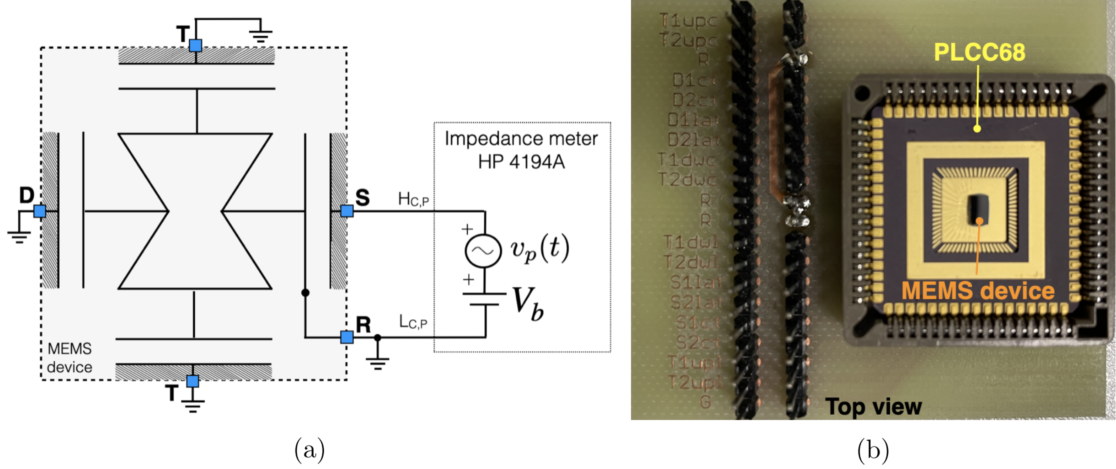


(a) (b)

Figure 3: (a) Block diagram of the setup employed for the static characterization of the auxetic MEMS device; (b) tailored printed circuit board containing the MEMS device bonded into a PLCC68 package.

configuration used to measure the capacitance $C_{SR}$ is reported in Figure 3a. Terminals $D$ and $T$ have been grounded while the sinusoidal probing signal $v_p(t)$ and the bias voltage $V_b$ have been applied between terminals $S$ and $R$. Note that the set of stators $T$, not reported in Figure 1c for the sake of simplicity, is located inside the top and bottom frames [9].

A similar configuration has been implemented to measure the capacitance $C_{DR}$, with $v_p(t)$ and $V_b$ applied between terminals $D$ and $R$, with $S$ and $T$ grounded. The root mean square (rms) amplitude and the frequency of the probing signal $v_p(t)$ have been set to 50 mV and 200 kHz, respectively to produce negligible time dependent electrostatic force and avoid mechanical resonances of the MEMS structure. The bias voltage $V_b$ has been tuned with a step size of 0.50 V (device A) and 0.25 V (device B), up to a maximum value of 12 V, to prevent the pull-in effect. Figure 3b shows the top view of the tailored printed circuit board (PCB) developed for the static characterization of the auxetic MEMS device bonded in the 68-pins plastic-leaded-chip-carrier (PLCC68) package.

### 3.2 Analytical capacitance-voltage model

In the hypothesis of uniform over etch and MEMS simmetric geometry, both the $F_S/F_D$ frames and the corresponding terminals $S/D$ are nominally equal. Since the gaps between the MEMS capacitors are much smaller than the effective dimensions of the parallel plates the capacitance $C$ between one of the two terminal $S/D$ and $R$ can be expressed, as first approximation, as

$$C = \frac{\varepsilon_0 A}{g - x}, \tag{8}$$

where $\varepsilon_0$ is the vacuum permittivity, $A$ is the total surface of the plates, $g$ is their initial gap and $x$ is the current relative displacement. The attractive force between the parallel plates can

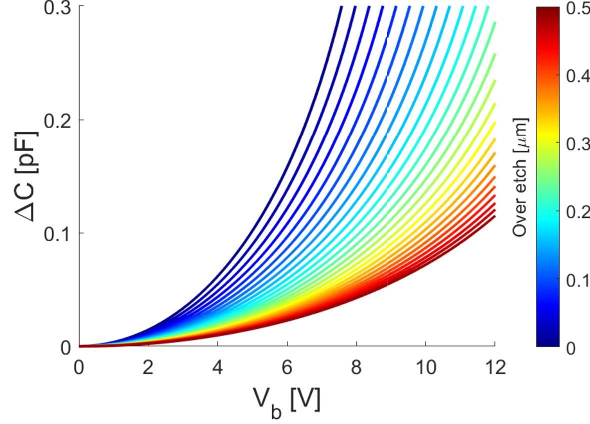


Figure 4: Capacitance-bias voltage curves between the terminals $S/D$ and $R$ for different values of the over etch

be evaluated through

$$F = \frac{1}{2}V^2\frac{dC}{dx} = \frac{1}{2}V^2\frac{\varepsilon_0 A}{(g-x)^2}, \tag{9}$$

where $V = V_b + v_p(t)$ is the voltage applied across the capacitance. As done in the experimental tests, setting a low rms amplitude of the probing signal $v_p(t)$ we can reasonably assume in (9) that $V^2 \simeq V_b^2$.

The capacitance-voltage relationship is obtained by enforcing the balance between the attractive forces between the plates and the restoring elastic force of the frames that can be expressed as $k_{eq}x$, being $k_{eq}$ the equivalent stiffness of the frame previously estimated through the homogenization of the inner deformable component of the MEMS filter. This provides the implicit relation

$$2\varepsilon_0 A g k_{eq}\Delta C = \left(\Delta C + \frac{\varepsilon_0 A}{g}\right)^3 V_b^2, \tag{10}$$

where $\Delta C = C - \varepsilon_0 A/g$. Note that both the equivalent stiffness $k_{eq}$ and the initial gap $g$ are functions of the over etch. The analytical capacitance-bias voltage relationship (10) between terminals $S/D$ and $R$ is plotted in Figure 4 for different values of the over etch.

### 3.3 Optimization procedure

The over etch identification is carried out on two MEMS devices (A and B) having the same nominal geometry.

The capacitance variations $\Delta C_{SR}^{exp}$ and $\Delta C_{DR}^{exp}$ at different bias voltage $V_b$ are first measured as explained in subsection 3.1. The experimental results are reported in Figure 5a and Figure 5b for device A and B respectively: blue dots refer to the capacitance $\Delta C_{SR}$, while the orange ones to $\Delta C_{DR}$.

Then, for each possible value of the over etch, corresponding to a particular $k_{eq}$, the analytical $\Delta C - V_b$ values are computed through eq. (10).

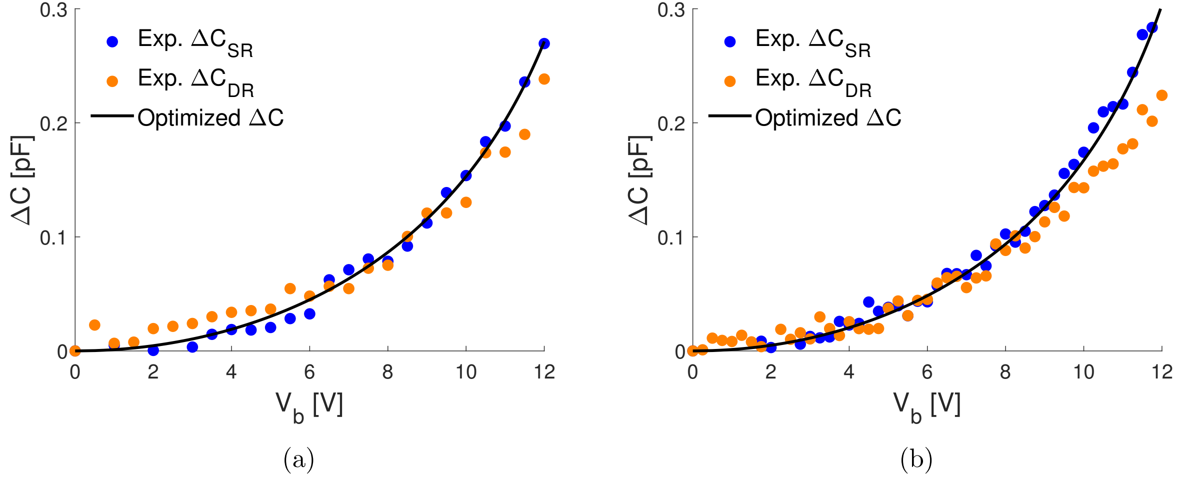


Figure 5: Experimental capacitance-bias voltage between terminals S and R (blue dots), and between terminals D and R (orange dots) for devices A (a) and B (b). The optimal analytical curves are shown in black.

The relative error reads

$$\mathcal{E} = \frac{||\Delta C_{SR}^{exp} - \Delta C||_{\ell^2}}{||\Delta C_{SR}^{exp}||_{\ell^2}} + \frac{||\Delta C_{DR}^{exp} - \Delta C||_{\ell^2}}{||\Delta C_{DR}^{exp}||_{\ell^2}}, \tag{11}$$

where $|| \diamond ||_{\ell^2}$ is the $\ell^2$ norm of $\diamond$. Note that a limited voltage interval, i.e. from 0V to 8V, is considered because high voltage will induce nonlinear phenomena, in contrast with the linearity hypothesis adopted in the computation of the equivalent stiffness through the homogenization technique. Large deformations of the MEMS mechanical structure which may occur at high voltage are indeed not considered in the present modelling strategy.

For both devices A and B, the relative error (11) is shown in Figure 6 as a function of the over etch. The dots represents the optimal over etches that minimize the relative error, which is 0.25 $\mu$m for device A, and 0.23 $\mu$m for device B. Both values are in very good agreement with the typical over etch values availble for the Thelma surface micromachining process [14] here employed for the fabrication of the MEMS filter.

The analytical capacitance versus voltage curves corresponding to the optimal values of over etch are shown in Figure 5a in Figure 5b by continuos black curves. They show a satisfactory agreement with experimental data.

## 4 CONCLUSIONS

In this work, we propose an efficient and time-saving tool for the over etch identification in a MEMS device.

Two-scale asymptotic homogenization is employed to characterize the static linear-elastic behaviour of a MEMS filter as a function of the over etch. The inner core of the mechanical structure is substituted with an equivalent homogeneous media and the equivalent stiffness of

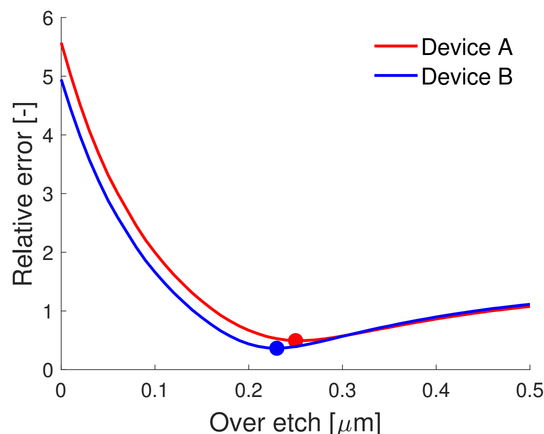


Figure 6: Relative error for devices A (red) and B (blue) against over etch

the MEMS frames is computed. Even with few cells, the homogenization approach has been shown to provide a good estimate of the real structural stiffness. By comparison with the full order numerical simulation of the real geometry in the case of zero over etch, the accuracy of the procedure and the strong reduction of the computational burden have been proved.

A simple analytical model able to describe the capacitance-bias voltage relationship between terminals $S/D$ and $R$ is derived and the over etch of the MEMS device is identified as the one that minimize the relative error between the experimental data and the analytical predictions. The resulting optimized $\Delta C - V_b$ analytical curves are in good agreement with the experimental observations for both the considered devices.

The proposed approach could be easily extended to different MEMS devices and for the inverse identification of further fabrication imperfections.

## REFERENCES

[1] Vikas Choudhary and Krzysztof Iniewski. *Mems: fundamental technology and applications*. CRC Press, 2017.

[2] Alberto Corigliano, Raffaele Ardito, Claudia Comi, Attilio Frangi, Aldo Ghisi, and Stefano Mariani. *Mechanics of Microsystems*. Wiley. ISBN 978–1–119–05383–5, 2018.

[3] Diana Nyyssonen and Robert D Larrabee. Submicrometer linewidth metrology in the optical microscope. *Journal of research of the National Bureau of Standards*, 92(3):187, 1987.

[4] Marc Gennat, Marco Meinig, Alexey Shaporin, Steffen Kurth, Christian Rembe, and Bernd Tibken. Determination of parameters with uncertainties for quality control in mems fabrication. *Journal of microelectromechanical systems*, 22(3):613–624, 2013.

[5] Maria F Pantano, Horacio D Espinosa, and Leonardo Pagnotta. Mechanical characterization of materials at small length scales. *Journal of Mechanical Science and technology*, 26(2):545–561, 2012.

[6] André Pineau, A Amine Benzerga, and Thomas Pardoen. Failure of metals iii: Fracture and fatigue of nanostructured metallic materials. *Acta Materialia*, 107:508–544, 2016.

[7] Ramin Mirzazadeh, Saeed Eftekhar Azam, and Stefano Mariani. Micromechanical characterization of polysilicon films through on-chip tests. *Sensors*, 16(8):1191, 2016.

[8] Ramin Mirzazadeh, Saeed Eftekhar Azam, and Stefano Mariani. Mechanical characterization of polysilicon mems: A hybrid tmcmc/pod-kriging approach. *Sensors*, 18(4), 2018.

[9] Valentina Zega, Alessandro Nastro, Marco Ferrari, Raffaele Ardito, Vittorio Ferrari, and Alberto Corigliano. An innovative auxetic electrically-tunable mems mechanical filter. In *2022 IEEE 35th International Conference on Micro Electro Mechanical Systems Conference (MEMS)*, pages 539–542, 2022.

[10] Valentina Zega, Alessandro Nastro, Marco Ferrari, Raffaele Ardito, Vittorio Ferrari, and Alberto Corigliano. Design, fabrication and experimental validation of a MEMS periodic auxetic structure. *Smart Materials and Structures*, 28(9):095011, aug 2019.

[11] Nikolai Sergeevich Bakhvalov and Grigory Panasenko. *Homogenisation: Averaging Processes in Periodic Media.* Kluwer Academic Publishers, 1989.

[12] Alain Bensoussan, Jacques-Louis Lions, and George Papanicolaou. *Asymptotic analysis for periodic structures.* North-Holland publishing company, 1978.

[13] Claudia Comi and Jean-Jacques Marigo. Homogenization Approach and Bloch-Floquet Theory for Band-Gap Prediction in 2D Locally Resonant Metamaterials. *Journal of Elasticity*, 139(1):61–90, 2020.

[14] Alberto Corigliano, Biagio De Masi, Attilio Frangi, Claudia Comi, Alberto Villa, and Mauro Marchi. Mechanical characterization of polysilicon through on-chip tensile tests. *Journal of Microelectromechanical Systems*, 13(2):200–219, 2004.